

A Comprehensive Analysis of the Pion-Photon Transition Form Factor Beyond the Leading Fock State

Tao Huang^{1,2*} and Xing-Gang Wu^{3†}

¹*CCAST(World Laboratory), P.O.Box 8730, Beijing 100080, P.R.China*

²*Institute of High Energy Physics, Chinese Academy of Sciences,
P.O.Box 918(4), Beijing 100039, P.R. China*

³*Institute of Theoretical Physics, Chinese Academy of Sciences,
P.O.Box 2735, Beijing 100080, P.R. China*

(Dated: August 10, 2018)

Abstract

We perform a comprehensive analysis of the pion-photon transition form factor $F_{\pi\gamma}(Q^2)$ involving the transverse momentum corrections with the present CLEO experimental data, in which the contributions beyond the leading Fock state have been taken into consideration. As is well-known, the leading Fock-state contribution dominates of $F_{\pi\gamma}(Q^2)$ at large momentum transfer (Q^2) region. One should include the contributions beyond the leading Fock state in small Q^2 region. In this paper, we construct a phenomenological expression to estimate the contributions beyond the leading Fock state based on its asymptotic behavior at $Q^2 \rightarrow 0$. Our present theoretical results agree well with the experimental data in the whole Q^2 region. Then, we extract some useful information of the pionic leading twist-2 distribution amplitude (DA) by comparing our results of $F_{\pi\gamma}(Q^2)$ with the CLEO data. By taking best fit, we have the DA moments, $a_2(\mu_0^2) = 0.002^{+0.063}_{-0.054}$, $a_4(\mu_0^2) = -0.022^{+0.026}_{-0.012}$ and all of higher moments, which are closed to the asymptotic-like behavior of the pion wavefunction.

PACS numbers: 13.40.Gp, 12.38.Bx, 12.39.Ki, 14.40.Aq

* email: huangtao@mail.ihep.ac.cn

† email: wuxg@itp.ac.cn

I. INTRODUCTION

The pion-photon transition form factor, which relates two photons with one lightest meson, is the simplest example for the perturbative application to exclusive processes. By neglecting k_\perp (the transverse momentum of the constitute quarks) relative to q_\perp (the transverse momentum of the virtual photon) in the hard-scattering amplitude, one can obtain the leading Fock-state formula [1]:

$$F_{\pi\gamma}(Q^2) = \frac{2f_\pi}{3Q^2} \int \frac{dx}{x} \phi_\pi(x, Q^2) \left[1 + \mathcal{O}\left(\alpha_s(Q^2), \frac{m^2}{Q^2}\right) \right], \quad (1)$$

where $Q^2 = -q^2$ stands for the momentum transfer in the process, the pion decay constant $f_\pi = 92.4 \pm 0.25$ MeV [2], and $\phi_\pi(x, Q^2)$ stands for the leading Fock-state pion distribution amplitude (DA) at the factorization scale $\mu^2 = Q^2$, which can be derived from the initial DA $\phi_\pi(x, \mu_0^2)$ (μ_0 stands for some hadronic scale) through QCD evolution. The initial DA is defined as

$$\phi_\pi(x, \mu_0^2) = \frac{2\sqrt{3}}{f_\pi} \int_{|\mathbf{k}_\perp|^2 \leq \mu_0^2} \frac{d^2\mathbf{k}_\perp}{16\pi^3} \Psi_{q\bar{q}}(x, \mathbf{k}_\perp). \quad (2)$$

Hence, the value of $Q^2 F_{\pi\gamma}(Q^2)$ tends to be a constant ($2f_\pi$) for asymptotic DA: $\phi_{as}(x, Q^2)|_{Q^2 \rightarrow \infty} = 6x(1-x)$. However, it has been argued that the k_\perp -dependence of the pion wavefunction can not be safely neglected at the end-point region $x_i \rightarrow 0, 1$ (x_i the momentum fraction of the constitute quarks in pion) and $Q^2 \sim$ a few GeV^2 . Under the light-cone (LC) pQCD approach, the leading contribution to $F_{\pi\gamma}(Q^2)$ that keeps the k_\perp -corrections in both the hard-scattering amplitude and the wavefunction can be written as [4, 5]:

$$F_{\pi\gamma}(Q^2) = 2\sqrt{3}(e_u^2 - e_d^2) \int_0^1 [dx] \int \frac{d^2\mathbf{k}_\perp}{16\pi^3} \Psi_{q\bar{q}}(x, \mathbf{k}_\perp) \times T_H(x, x', \mathbf{k}_\perp), \quad (3)$$

where $[dx] = dx dx' \delta(1-x-x')$, $e_{u,d}$ are the quark charges in unites of e , $\Psi_{q\bar{q}}(x, \mathbf{k}_\perp)$ stands for the leading Fock-state wavefunction and the hard-scattering amplitude $T_H(x, x', \mathbf{k}_\perp)$ takes the form,

$$T_H(x, x', \mathbf{k}_\perp) = \frac{\mathbf{q}_\perp \cdot (x' \mathbf{q}_\perp + \mathbf{k}_\perp)}{\mathbf{q}_\perp^2 (x' \mathbf{q}_\perp + \mathbf{k}_\perp)^2} + (x \leftrightarrow x'). \quad (4)$$

With the help of Eqs.(3,4), Ref.[5] performed a careful analysis of the quark transverse-momentum effect to $F_{\pi\gamma}(Q^2)$. They pointed out that the transverse-momentum dependence in both the numerator and the denominator of the hard-scattering amplitude are of the same importance and should be considered consistently. Similar improved treatment has

also been done in Refs.[6, 7, 8, 9, 10, 11, 12]. It was shown that pQCD can give the correct prediction for the pion-photon transition form factor that is consistent with the present experimental data by keeping the k_{\perp} -dependence in both the hard-scattering amplitude and the pion wavefunction and by properly choosing of the pion wavefunction.

It should be noted that Eqs.(1,3) were obtained by assuming the leading Fock-state dominance. This approximation is valid only for large Q^2 region and one can not expect that these expressions can describe the present experimental data well in low Q^2 region. Refs.[13, 14] show that the approximation of the leading Fock-state dominance to the pion electro-magnetic form factor is valid as $Q^2 \gtrsim 4 \text{ GeV}^2$, which is improved to be $Q^2 \gtrsim 1 \text{ GeV}^2$ by including the next-to-leading order (NLO) contribution [15, 16]. A similar discussion has been done in Ref.[5] for the pion-photon transition form factor. These references tell us that one should take into account the higher Fock states' contributions as $Q^2 < a \text{ few GeV}^2$. In fact, it has been shown that the expression (3) gives half contribution to $F_{\pi\gamma}(Q^2)$ as one extends it to $Q^2 = 0$ [4]. It means that the leading Fock state contributes to $F_{\pi\gamma}(0)$ only half and the remaining half should be come from the higher Fock states. Both contributions from the leading Fock state and the higher Fock states are needed to get the correct $\pi^0 \rightarrow \gamma\gamma$ rate [4]. Any attempt that involves only the leading Fock-state contribution to explain both the $\pi^0 \rightarrow \gamma\gamma$ rate and the pion-photon transition form factor for low Q^2 region is incorrect. It should be pointed out that the above conclusion does not contradict with that of Ref.[17], where with the help of an “effective” two-body wavefunction that includes the soft contributions from the higher Fock components, the authors pointed that the contributions corresponding to higher Fock states in a hard region appear as radiative corrections and are suppressed by powers of $(\alpha_s/\pi) \sim 10\%$.

In this paper, we will take the contributions from both the leading Fock state and the higher Fock states into consideration. Especially, we will discuss how to consider the contributions beyond the leading Fock state at low Q^2 region and give a careful analysis of the pion-photon transition form factor in the whole Q^2 region. Furthermore, we can learn more information of the leading twist-2 DA from the present CLEO data, since the pion-photon transition form factor in the simplest exclusive process only involves one pion and the contributions from the higher twist structures and higher helicity states are highly suppressed (at least by $1/Q^4$) in comparison to the leading twist-2 pion wavefunction. In the present paper, we will not include the NLO contribution into our formulae. Since we need a full

NLO result in order to be consistent with our present calculation technique, in which the effects caused by the transverse-momentum dependence in the hard-scattering amplitude and the pion wavefunction and by the Sudakov factor should be fully considered, however such a full NLO calculation is not available at the present ¹.

The paper is organized as follows. In Sec.II, we analyze the contributions to $F_{\pi\gamma}(Q^2)$ beyond the leading Fock state at low Q^2 region under the LC pQCD approach and give a complete expression for $F_{\pi\gamma}(Q^2)$ in the whole Q^2 region. In Sec.III, we discuss what we can learn of the pionic leading Fock-state wavefunction/DA in comparison with CLEO experimental data. Some further discussion and comments are made in Sec.IV. The last section is reserved for a summary.

II. AN EXPRESSION OF $F_{\pi\gamma}(Q^2)$ FROM ZERO TO LARGE Q^2 REGION

First, we give a brief review of the LC formalism [1, 19, 20]. The LC formalism provides a convenient framework for the relativistic description of hadrons in terms of quark and gluon degrees of freedom and for the application of pQCD to exclusive processes. The LC Fock-state expansion of wavefunction provides a precise definition of the parton model and a general method to calculate the hadronic matrix element. As for the pion wavefunction, its Fock-state expansion is

$$|\pi\rangle = \sum |q\bar{q}\rangle \Psi_{q\bar{q}} + \sum |q\bar{q}g\rangle \Psi_{q\bar{q}g} + \cdots, \quad (5)$$

where the Fock-state wavefunctions $\Psi_n(x_i, \mathbf{k}_{\perp i}, \lambda_i)$ ($n = 2, 3, \cdots$) satisfy the normalization condition

$$\sum_{n, \lambda_i} \int [dx d^2\mathbf{k}_{\perp}]_n |\Psi_n(x_i, \mathbf{k}_{\perp i}, \lambda_i)|^2 = 1, \quad (6)$$

with $[dx d^2\mathbf{k}_{\perp}]_n = 16\pi^3 \delta(1 - \sum_{i=1}^n x_i) \delta^2(\sum_{i=1}^n \mathbf{k}_{\perp i}) \prod_{i=1}^n \left[\frac{dx_i d^2\mathbf{k}_{\perp i}}{16\pi^3} \right]$. λ_i is the helicity of the constituents and n stands for all Fock states, e.g. $\Psi_2 = \Psi_{q\bar{q}}$. It should be pointed out that we have $\int [dx d^2\mathbf{k}_{\perp}]_2 \sum_{\lambda_i} |\Psi_{q\bar{q}}(x_i, \mathbf{k}_{\perp i}, \lambda_i)|^2 < 1$ for the leading Fock state.

The pion-photon transition form factor is connected with the $\pi^0\gamma\gamma^*$ vertex in the ampli-

¹ The present NLO result is derived without considering the transverse-momentum dependence in the hard-scattering amplitude and the wavefunction, see e.g. Refs.[9, 10, 15, 16, 18].

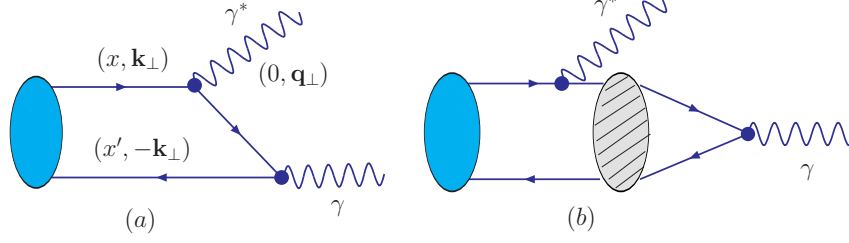


FIG. 1: Typical diagrams that contribute to the pion-photon transition form factor $F_{\pi\gamma}(Q^2)$, where $x' = (1 - x)$. The rightmost shaded oval with a slant pattern stands for the strong interactions.

tude of $e\pi \rightarrow e\gamma$ as

$$\Gamma_\mu = -ie^2 F_{\pi\gamma}(Q^2) \epsilon_{\mu\nu\alpha\beta} P^\mu \epsilon^\alpha q^\beta, \quad (7)$$

where P and q are the momenta of the incident pion and the virtual photon respectively, and ϵ is the polarization vector of the final on-shell photon. To simplify the hard-scattering amplitude, we adopt the Drell-Yan-West assignment at the ‘infinite-momentum’ frame [21]: $q = (q_+, q_-, \mathbf{q}_\perp) = (0, |\mathbf{q}_\perp|^2/P^+, \mathbf{q}_\perp)$ and $P = (P^+, P^-, \mathbf{P}_\perp) = (1, 0, \mathbf{0}_\perp)$, where P^+ is arbitrary because of Lorentz invariance and it is taken to be 1 for convenience. Then $F_{\pi\gamma}$ is given by [1]

$$F_{\pi\gamma}(Q^2) = \frac{\Gamma^+}{-ie(\epsilon_\perp \times \mathbf{q}_\perp)}, \quad (8)$$

where $Q^2 = -q^2 = |\mathbf{q}_\perp|^2$, $\epsilon = (0, 0, \epsilon_\perp)$, $\epsilon_\perp \cdot \mathbf{q}_\perp = 0$ and $\epsilon_\perp \times \mathbf{q}_\perp = \epsilon_{\perp 1} q_{\perp 2} - \epsilon_{\perp 2} q_{\perp 1}$.

As illustrated in Fig.(1), there are two basic types of contribution to $F_{\pi\gamma}(Q^2)$, i.e. $F_{\pi\gamma}^{(V)}(Q^2)$ and $F_{\pi\gamma}^{(NV)}(Q^2)$. $F_{\pi\gamma}^{(V)}(Q^2)$ comes from Fig.(1a), which involves the direct annihilation of $(q\bar{q})$ -pair into two photons, i.e. the leading Fock-state contribution that dominates the large Q^2 contribution. $F_{\pi\gamma}^{(NV)}(Q^2)$ comes from Fig.(1b), in which one photon coupling ‘inside’ the pion wavefunction, i.e. strong interactions occur between the photon interactions that is related to the higher Fock states’ contributions. An interpretation for $F_{\pi\gamma}^{(NV)}(Q^2)$ can be given under the operator product expansion (OPE) approach [17]. Under the OPE approach [22], the nonperturbative aspects of the hadron dynamics are described by matrix elements of local operators. In particular, the longitudinal momentum distribution is related to the lowest-twist composite operators. While by taking into account the transverse-momentum effects, one needs to consider matrix elements of higher-twist composite operators in which some of the covariant derivatives appear in a contracted form like

$D^2 = D_\mu D^\mu$. By using the equation of motion for the light quark, $\gamma^\mu D_\mu q = 0$, one can convert a two-body quark-antiquark operator $\bar{q}\{\gamma_{\mu_1} D_{\mu_2} \dots D_{\mu_n}\} D^2 q$ into the “three-body” operator $\bar{q}\{\gamma_{\mu_1} D_{\mu_2} \dots D_{\mu_n}\}(\sigma^{\mu\nu} G_{\mu\nu})q$ with an extra gluonic field $G_{\mu\nu}$ being involved, which is just related to the higher Fock state of pion.

The first type of contribution $F_{\pi\gamma}^{(V)}(Q^2)$ stands for the conventional leading Fock-state contribution. Under the LC pQCD approach and by keeping the full k_T -dependence in both the hard-scattering amplitude and the wavefunction, the expression for $F_{\pi\gamma}^{(V)}(Q^2)$ is the one that is given in Eqs.(3,4), where the terms involving the higher helicity states ($\lambda_1 + \lambda_2 = \pm 1$, λ_i stands for the corresponding helicity of the two constitute quarks of pion) and the higher twist structures of the pion wavefunction are not explicitly written. Since by direct calculating, one may observe that the contributions from the higher helicity states and the higher twist structures of the pion wavefunction are suppressed by at least $1/Q^4$ to that of the usual helicity state ($\lambda_1 + \lambda_2 = 0$) of the leading Fock state, which agrees with the discussion made in Ref.[9]².

As for the second type of contribution $F_{\pi\gamma}^{(NV)}(Q^2)$, it is difficult to be calculated in any Q^2 region. If treating the photon vertex in Fig.(1b) as a vector meson dressed photon vertex, Fig.(1b) can be calculated approximately under the vector meson dominance (VMD) approach, see e.g. Ref.[23] for a review and Refs.[24, 25] for an explicit VMD calculation of the pion electro-magnetic form factor. By adopting the VMD approach to approximate Fig.(1b), one needs to introduce some undetermined coupling factor either for VMD1 or VMD2 formulation [23], which together with the undetermined parameters in the pion wavefunction can not be definitely determined by the CLEO experimental data of the pion transition form factor only and some other constraints should also be taken into consideration, e.g. the constraint from the experimental value for the pion charge radius or the constraint from the experimental value for the pion electro-magnetic form factor. In fact, one usually takes the value of $F_{\pi\gamma}(Q^2) = F_{\pi\gamma}^{(V)}(Q^2) + F_{\pi\gamma}^{(NV)}(Q^2)$ derived from the VMD approach to be in a simple monopole form [26], i.e. $F_{\pi\gamma}(Q^2) = 1/[4\pi^2 f_\pi(1 + Q^2/m_\rho^2)]$, with the ρ -meson mass m_ρ serves as a parameter determined by the pion charge radius. For the purpose of extracting some useful information of the pion wavefunction from the CLEO experimental data,

² The present condition is quite different from the case of pion electro-magnetic form factor, where the contributions from the higher helicity states and higher twist structures are only suppressed by $1/Q^2$ and then they can provide sizable contribution in the intermediate Q^2 region [37, 38].

we adopt the method raised by Ref.[4] to deal with $F_{\pi\gamma}^{(NV)}(Q^2)$ ³.

As stated in Ref.[4], around the region of $Q^2 \sim 0$, since the wavelength of the photon ‘inside’ the pion wavefunction $\sim 1/m_\pi$ is assumed to be much larger than the pion radius $1/\lambda$ (λ is some typical hadronic scale ~ 1 GeV), we can treat such photon (nearly on-shell) as an external field which is approximately constant throughout the pion volume. And then, a fermion in a constant external field is modified only by a phase, i.e. $S_A(x-y) = e^{-ie(y-x)\cdot A} S_F(x-y)$. Consequently, the lowest $q\bar{q}$ -wavefunction for the pion is modified only by a phase $e^{-iey\cdot A}$, where y is the $q\bar{q}$ -separation. Transforming such phase into the momentum space and applying it to the wavefunction, the second contribution $F_{\pi\gamma}^{(NV)}(Q^2)$ at $\mathbf{q}_\perp \rightarrow 0$ can be simplified to

$$F_{\pi\gamma}^{(NV)}(Q^2)|_{\mathbf{q}_\perp \rightarrow 0} = \frac{-2}{\sqrt{3}Q^2} \int [dx] \int \frac{d^2\mathbf{k}_\perp}{16\pi^3} \left\{ \frac{(\mathbf{k}_\perp \times \mathbf{q}_\perp)^2}{(x'\mathbf{q}_\perp + \mathbf{k}_\perp)^2} \left[\frac{\partial}{\partial k_\perp^2} \Psi_{q\bar{q}}(x, \mathbf{k}_\perp) \right] + (x \leftrightarrow x') \right\}, \quad (9)$$

where $[dx] = dx dx' \delta(1-x-x')$ and $k_\perp = |\mathbf{k}_\perp|$. Eq.(9) gives the expression for $F_{\pi\gamma}^{(NV)}(Q^2)$ at $Q^2 \rightarrow 0$. Here different from Ref.[4], all \mathbf{q}_\perp -terms that are necessary to obtain its first derivative over Q^2 are retained and the relation $(\epsilon_\perp \times \mathbf{q}_\perp)(\mathbf{k}_\perp \times \mathbf{q}_\perp) = Q^2(\epsilon_\perp \cdot \mathbf{k}_\perp)$ is implicitly adopted. After doing the integration over \mathbf{k}_\perp , one can easily find that

$$F_{\pi\gamma}^{(NV)}(0) = F_{\pi\gamma}^{(V)}(0) = \frac{1}{8\sqrt{3}\pi^2} \int dx \Psi_{q\bar{q}}(x, \mathbf{0}_\perp), \quad (10)$$

which means that the leading Fock state contributes to $F_{\pi\gamma}(0) = F_{\pi\gamma}^{(V)}(0) + F_{\pi\gamma}^{(NV)}(0)$ only half, and one can get the correct rate of the process $\pi^0 \rightarrow \gamma\gamma$ provided that the two basic contributions $F_{\pi\gamma}^{(V)}(0)$ and $F_{\pi\gamma}^{(NV)}(0)$ are considered simultaneously. By taking into account the PCAC prediction [27], $F_{\pi\gamma}(0) = 1/(4\pi^2 f_\pi)$, one can obtain the important constraint of the pion wavefunction, i.e.

$$\int_0^1 dx \Psi_{q\bar{q}}(x, \mathbf{k}_\perp = 0) = \frac{\sqrt{3}}{f_\pi}. \quad (11)$$

Without loss of generality, we can assume that the pion wavefunction depending on \mathbf{k}_\perp through k_\perp^2 only, i.e. $\Psi_{q\bar{q}}(x, \mathbf{k}_\perp) = \Psi_{q\bar{q}}(x, k_\perp^2)$ ⁴. Then $F_{\pi\gamma}^{(V)}(Q^2)$ (Eq.(3)) can be simplified

³ A careful VMD calculation of the pion transition form factor along the line of Refs.[24, 25] can be used as a cross check of our results, however it is out of the range of the present paper.

⁴ The spin-space Wigner rotation might change this property for the higher helicity components as shown in Ref.[28]. Since the higher helicity components’ contribution are highly suppressed for the present case, we do not take this point into consideration in the present paper.

after doing the integration over the azimuth angle as [9]

$$F_{\pi\gamma}^{(V)}(Q^2) = \frac{1}{4\sqrt{3}\pi^2} \int_0^1 \frac{dx}{xQ^2} \int_0^{x^2Q^2} \Psi_{q\bar{q}}(x, k_\perp^2) dk_\perp^2. \quad (12)$$

Similarly, for the first derivative of $F_{\pi\gamma}^{(NV)}(Q^2)$ over Q^2 , we have

$$F_{\pi\gamma}^{(NV)'}(Q^2)|_{Q^2 \rightarrow 0} = \frac{1}{8\sqrt{3}\pi^2} \left[\frac{\partial}{\partial Q^2} \int_0^1 \int_0^{x^2Q^2} \left(\frac{\Psi_{q\bar{q}}(x, k_\perp^2)}{x^2Q^2} \right) dx dk_\perp^2 \right]_{Q^2 \rightarrow 0}. \quad (13)$$

Furthermore, the leading twist-2 pion DA at the factorization scale μ can be simplified as

$$\phi_\pi(x, \mu^2) = \frac{\sqrt{3}}{8\pi^2 f_\pi} \int_0^{\mu^2} \psi_{q\bar{q}}(x, k_\perp^2) dk_\perp^2. \quad (14)$$

With the help of Eqs.(12,14), $F_{\pi\gamma}^{(V)}(Q^2)$ can be rewritten as

$$F_{\pi\gamma}^{(V)}(Q^2) = \frac{2f_\pi}{3Q^2} \int_0^1 \frac{dx}{x} \phi_\pi(x, x^2Q^2). \quad (15)$$

Note that Eq.(15) is different from Eq.(1) only by replacing $\phi_\pi(x, Q^2)$ to $\phi_\pi(x, x^2Q^2)$. It means that the leading contribution to $F_{\pi\gamma}(Q^2)$ as shown in Eq.(3), which was given by keeping the k_\perp -corrections in both the hard-scattering amplitude and the pion wavefunction, can be equivalently obtained by setting the upper limit for the integral of the pion DA to be $[\mu^2 = x^2Q^2]$. The x -dependent upper limit $[x^2Q^2]$ affects $F_{\pi\gamma}^{(V)}(Q^2)$ from the small to intermediate Q^2 region, and such effect will be more explicit for a wider pion DA, such as the CZ (Chernyak-Zhitnitsky)-like model [3] that emphasizes the end-point region in a strong way, as has been discussed in Ref.[5]. In the literature, the pion DA is usually expanded in Gegenbauer polynomial expansion as

$$\phi_\pi(x, \mu^2) = \phi_{as}(x) \cdot \left[1 + \sum_{n=1}^{\infty} a_{2n}(\mu^2) C_{2n}^{3/2}(\xi) \right], \quad (16)$$

where $\xi = (2x - 1)$, $C_n^{3/2}(\xi)$ are Gegenbauer polynomials and $a_{2n}(\mu^2)$, the so called Gegenbauer moments, are hadronic parameters that depend on the factorization scale μ . The Gegenbauer moments $a_{2n}(\mu^2)$ can be related to $a_{2n}(\mu_0^2)$ with the help of QCD evolution, where μ_0 stands for some fixed low energy scale. To leading logarithmic accuracy, we have [10, 29]

$$a_{2n}(\mu^2) = a_{2n}(\mu_0^2) \left(\frac{\alpha_s(\mu^2)}{\alpha_s(\mu_0^2)} \right)^{\gamma_0^{(2n)}/(2\beta_0)}, \quad (17)$$

where $\beta_0 = 11 - 2n_f/3$, $\alpha_s(Q^2) = 4\pi/[\beta_0 \ln(Q^2/\Lambda_{QCD}^2)]$ and the one-loop anomalous dimension is

$$\gamma_0^{(2n)} = 8C_F \left(\psi(2n+2) + \gamma_E - \frac{3}{4} - \frac{1}{(2n+1)(2n+2)} \right). \quad (18)$$

We need to know $\phi_\pi(x, x^2 Q^2)$ and $F_{\pi\gamma}^{(NV)}(Q^2)$ to get the whole behavior of $F_{\pi\gamma}(Q^2)$, i.e.

$$F_{\pi\gamma}(Q^2) = F_{\pi\gamma}^{(V)}(Q^2) + F_{\pi\gamma}^{(NV)}(Q^2), \quad (19)$$

where $F_{\pi\gamma}^{(V)}(Q^2)$ is determined by $\phi_\pi(x, x^2 Q^2)$. The $\phi_\pi(x, x^2 Q^2)$ depends on the behavior of $\Psi_{q\bar{q}}(x, \mathbf{k}_\perp)$ and its Gegenbauer moments can not be directly obtained from the QCD evolution equation (17), since $[x^2 Q^2]$ can be very small and then the Landau ghost singularity in the running coupling α_s can not be avoided. As for $F_{\pi\gamma}^{(NV)}(Q^2)$, Eq.(9) presents an expression only at $Q^2 \sim 0$ region, and it can not be directly extended to the whole Q^2 region. Ref.[9] did an attempt to understand the higher Q^2 behavior of $F_{\pi\gamma}(Q^2)$ within the QCD sum rule approach, i.e. they raised a simple picture: the sum over the soft $\bar{q}G \cdots Gq$ Fock components is dual to $q\bar{q}$ -state generated by the local axial vector current. Furthermore, they raised an ‘effective’ two-body pion wavefunction that includes all soft contributions from the higher Fock states based on the QCD sum rule analysis and then calculated $F_{\pi\gamma}(Q^2)$ within the pQCD approach. Here we will not adopt such an ‘effective’ pion wavefunction to do the calculation, since we plan to extract some information for the leading Fock-state wavefunction by comparing with the CLEO experimental data.

In order to construct an expression of $F_{\pi\gamma}^{(NV)}(Q^2)$ in the whole Q^2 region, we require the following conditions at least:

- i) $F_{\pi\gamma}^{(NV)}(Q^2)|_{Q^2=0}$ should be given by Eq.(10).
- ii) $F_{\pi\gamma}^{(NV)'}(Q^2)|_{Q^2 \rightarrow 0} = \partial F_{\pi\gamma}^{(NV)}(Q^2)/\partial Q^2|_{Q^2 \rightarrow 0}$ should be derived from Eq.(9).
- iii) $\frac{F_{\pi\gamma}^{(NV)}(Q^2)}{F_{\pi\gamma}^{(V)}(Q^2)} \rightarrow 0$, as $Q^2 \rightarrow \infty$.

One can construct a phenomenological model for $F_{\pi\gamma}^{(NV)}(Q^2)$ that satisfies the above three requirements. It is natural to assume the following form

$$F_{\pi\gamma}^{(NV)}(Q^2) = \frac{\alpha}{(1 + Q^2/\kappa^2)^2}, \quad (20)$$

where κ and α are two parameters that can be determined by the above conditions (i,ii), i.e.

$$\alpha = \frac{1}{2} F_{\pi\gamma}(0) = \frac{1}{8\pi^2 f_\pi} \quad (21)$$

and

$$\kappa = \sqrt{-\frac{F_{\pi\gamma}(0)}{\frac{\partial}{\partial Q^2} F_{\pi\gamma}^{(NV)}(Q^2)|_{Q^2 \rightarrow 0}}}. \quad (22)$$

As for the phenomenological formula (20), it is easy to find that $F_{\pi\gamma}^{(NV)}(Q^2)$ will be suppressed by $1/Q^2$ to $F_{\pi\gamma}^{(V)}(Q^2)$ in the limit $Q^2 \rightarrow \infty$. Such a $1/Q^2$ -suppression is reasonable, since the

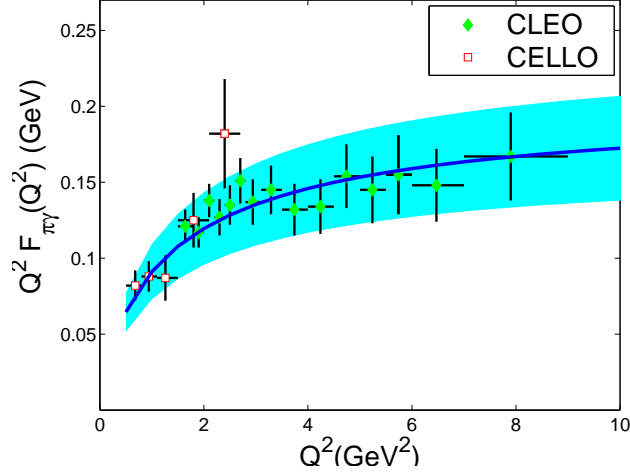


FIG. 2: The fitting curve (the solid line) for $Q^2 F_{\pi\gamma}(Q^2)$ from the CLEO and CELLO experimental data [30, 31], where a shaded band shows its uncertainty of $\pm 20\%$.

phenomenological expression (20) can be regarded as a summed up effect of all the high twist structures of the pion wavefunction, even though each higher twist structure is suppressed by at least $1/Q^4$ [9].

III. CALCULATED RESULTS WITH THE MODEL WAVEFUNCTION

The CLEO collaboration has measured the $\gamma\gamma^* \rightarrow \pi^0$ form factor [30]. In this experiment, one of the photons is nearly on-shell and the other one is highly off-shell, with a virtuality in the range $1.5 \text{ GeV}^2 - 9.2 \text{ GeV}^2$ [30]. There also exists older experimental results obtained by the CELLO collaboration [31]. By comparing the theoretical prediction with the experimental results, it provides us a chance to determine a precise form for the leading Fock-state pion wavefunction. Similar attempt to determine the pion DA has been done in literature [32, 33], e.g. Ref.[32] used the QCD light-cone sum rule analysis of the CLEO data to obtain parameters of the pion DA. In Fig.2, we show the fitting curve for $Q^2 F_{\pi\gamma}(Q^2)$ (derived by using the conventional χ^2 -fitting method described in Ref.[34] with slight change to make the curve more smooth) from the CLEO and CELLO experimental data, i.e. under the region of $Q^2 \in [0.5, 10.0] \text{ GeV}^2$, $Q^2 F_{\pi\gamma}(Q^2) \simeq [8.81 \times 10^{-7}(Q'^2)^5 - 4.78 \times 10^{-5}(Q'^2)^4 + 9.96 \times 10^{-4}(Q'^2)^3 - 1.01 \times 10^{-2}(Q'^2)^2 + 5.29 \times 10^{-2}(Q'^2) + 4.48 \times 10^{-2}] \text{ GeV}$ with the dimensionless

parameter $Q'^2 = Q^2/\text{GeV}^2$. Here the shaded band shows its $\pm 20\%$ uncertainty⁵. In fact, most of the results given in literature, e.g. Refs. [5, 6, 7, 8, 9, 10, 11, 32], are mainly within such region. The shaded band (region) for $Q^2 F_{\pi\gamma}(Q^2)$ can be regarded as a constraint to determine the pion wavefunction, i.e. the values of the parameters in the pion wavefunction should make $Q^2 F_{\pi\gamma}(Q^2)$ within the region of the shaded band as shown in Fig.(2).

Now we are in position to calculate the pion-photon transition form factor with the help of Eq.(19). As has been discussed in the last section, we need to know the leading Fock-state pion wavefunction $\Psi_{q\bar{q}}(x, \mathbf{k}_\perp)$ so as to derive $\phi_\pi(x, x^2 Q^2)$ that is necessary for $F_{\pi\gamma}^{(V)}(Q^2)$ and to derive the values of α and κ for $F_{\pi\gamma}^{(NV)}(Q^2)$. Several non-perturbative approaches have been developed to provide the theoretical predictions for the hadronic wavefunction. One useful way is to use the approximate bound-state solution of a hadron in terms of the quark model as the starting point for modeling the hadronic wavefunction. The Brodsky-Huang-Lepage (BHL) prescription [4] for the hadronic wavefunction is obtained in this way by connecting the equal-time wavefunction in the rest frame and the wavefunction in the infinite momentum frame. In the present paper, we shall adopt the revised LC harmonic oscillator model as suggested in Ref.[28] to do our calculation, which is constructed based on the BHL-prescription. As discussed in the above section, the contribution from the higher helicity states ($\lambda_1 + \lambda_2 = \pm 1$) is highly suppressed in comparison to that of the usual helicity state ($\lambda_1 + \lambda_2 = 0$), so we only write down the form of the pion wavefunction for the usual helicity state:

$$\Psi_{q\bar{q}}(x, \mathbf{k}_\perp) = \varphi_{\text{BHL}}(x, \mathbf{k}_\perp) \chi^K(x, \mathbf{k}_\perp) = A \exp \left[-\frac{\mathbf{k}_\perp^2 + m^2}{8\beta^2 x(1-x)} \right] \chi^K(x, \mathbf{k}_\perp), \quad (23)$$

with the normalization constant A , the harmonic scale β and the quark mass m to be determined. The spin-space wavefunction $\chi^K(x, \mathbf{k}_\perp)$ can be written as [28], $\chi^K(x, \mathbf{k}_\perp) = m/\sqrt{m^2 + k_\perp^2}$ with $k_\perp = |\mathbf{k}_\perp|$. By taking the BHL-like wavefunction (23), $F_{\pi\gamma}^{(V)}(Q^2)$ (Eq.(12)) can be simplified as

$$F_{\pi\gamma}^{(V)}(Q^2) = \int_0^1 dx \left\{ \frac{Am\beta}{\sqrt{6}\pi^{3/2}Q^2} \sqrt{\frac{x'}{x}} \left(\text{Erf} \left[\frac{\sqrt{m^2 + x^2 Q^2}}{2\beta\sqrt{2xx'}} \right] - \text{Erf} \left[\frac{\sqrt{m^2}}{2\beta\sqrt{2xx'}} \right] \right) \right\}, \quad (24)$$

where the error function $\text{Erf}(x)$ is defined as $\text{Erf}(x) = \frac{2}{\sqrt{\pi}} \int_0^x e^{-t^2} dt$. And similarly, for the limiting behaviors of $F_{\pi\gamma}^{(NV)}(Q^2)$ that are necessary to determine the parameters α and κ ,

⁵ It is so chosen since the sum of the statistical and systematic errors of the experimental data is $\lesssim \pm 20\%$ [30, 31].

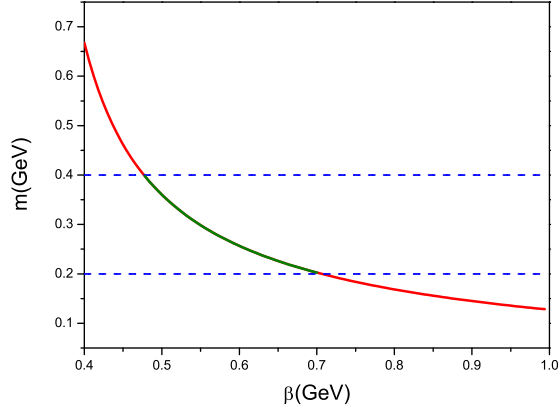


FIG. 3: The curve for the value of m versus β , which shows that if m is in the reasonable region $[0.20 \text{ GeV}, 0.40 \text{ GeV}]$ then $\beta \in [0.48 \text{ GeV}, 0.70 \text{ GeV}]$.

we obtain

$$F_{\pi\gamma}^{(NV)}(Q^2)|_{Q^2 \rightarrow 0} = \frac{A}{8\sqrt{3}\pi^2} \int_0^1 \exp\left[-\frac{m^2}{8\beta^2 xx'}\right] dx \quad (25)$$

and

$$F_{\pi\gamma}^{(NV)'}(Q^2)|_{Q^2 \rightarrow 0} = \frac{-A}{128\sqrt{3}m^2\pi^2\beta^2} \int_0^1 \frac{x}{x'}(m^2 + 4xx'\beta^2) \exp\left[-\frac{m^2}{8\beta^2 xx'}\right] dx, \quad (26)$$

where $x' = 1 - x$.

The possible range for the parameters of the pion wavefunction (23) can be derived by comparing our result of $Q^2 F_{\pi\gamma}(Q^2)$ with the experimental data. Further more, the model wavefunction should satisfy the following two conventional constraints:

- The pion wavefunction satisfies the normalization that is derived from the $\pi \rightarrow \mu\nu$ process [4, 28]:

$$\int_0^1 dx \int_{|\mathbf{k}_\perp|^2 < \mu^2} \frac{d^2\mathbf{k}_\perp}{16\pi^3} \Psi_{q\bar{q}}(x, \mathbf{k}_\perp) = \frac{f_\pi}{2\sqrt{3}}, \quad (27)$$

where the cut $|\mathbf{k}_\perp|^2 < \mu^2$ has been explicitly included. Substituting the pion wavefunction (23) into Eq.(27), we obtain

$$\int_0^1 \frac{Am\beta\sqrt{x(1-x)}}{4\sqrt{2}\pi^{3/2}} \left(\text{Erf}\left[\sqrt{\frac{m^2 + \mu^2}{8\beta^2 x(1-x)}}\right] - \text{Erf}\left[\sqrt{\frac{m^2}{8\beta^2 x(1-x)}}\right] \right) dx = \frac{f_\pi}{2\sqrt{3}}. \quad (28)$$

As for the model wavefunction (23), it can be found that the contribution from higher $|\mathbf{k}_\perp|$ region to the wavefunction normalization drops down exponentially, e.g. by taking

reasonable values for the wavefunction parameters, the wavefunction in the region of $|\mathbf{k}_\perp| > 1$ GeV only contributes about 5% to its total normalization, which changes to be less than 1% in the region of $|\mathbf{k}_\perp| > 2$ GeV. For clarity, we take the factorization scale μ to be $\mu = \mu_0 \simeq 2$ GeV, where μ_0 stands for some hadronic scale that is of order $\mathcal{O}(1$ GeV) and the choice of $\mu_0 \simeq 2$ GeV is also close to the virtuality of the photons in the central region of the experimental data. By taking $1 \text{ GeV} \leq \mu_0 \leq 2 \text{ GeV}$ that is of order $\mu_0 \sim \mathcal{O}(1 \text{ GeV})$, we find that the following results will be slightly changed, especially for the DA moments due to the fact that they satisfy the QCD evolution equation (17) within errors. A similar discussion on this point can also be found in Ref.[32]. Furthermore, one can safely take $\mu = \infty$ to simplify the calculation due to the smallness of the wavefunction in the region of $|\mathbf{k}_\perp| > \mu_0 = 2 \text{ GeV}$.

- Another constraint, as shown in Eq.(11), for the pion wavefunction can be derived from $\pi^0 \rightarrow \gamma\gamma$ decay amplitude [4], which can be further simplified as

$$\int_0^1 A \exp \left[-\frac{m^2}{8\beta^2 x(1-x)} \right] dx = \frac{\sqrt{3}}{f_\pi}. \quad (29)$$

Solving Eqs.(28,29) numerically, we obtain an approximate relation for m and β , i.e.

$$6.00 \frac{m\beta}{f_\pi^2} \cong 1.12 \left(\frac{m}{\beta} + 1.31 \right) \left(\frac{m}{\beta} + 5.47 \times 10^1 \right), \quad (30)$$

which shows that the value of m is decreased with the increment of β . More explicitly, Fig.(3) shows that β should be within the region of $[0.48 \text{ GeV}, 0.70 \text{ GeV}]$ so as to restrict m within the reasonable region of $[0.20 \text{ GeV}, 0.40 \text{ GeV}]$.

Before doing the numerical calculation for $F_{\pi\gamma}(Q^2)$, we note a naive interpolation formula for both perturbative and non-perturbative regions has been proposed by Brodsky and Lepage [1], which is similar to the monopole form derived from VMD approach [26], i.e.

$$F_{\pi\gamma}^{BL}(Q^2) = \frac{1}{4\pi^2 f_\pi (1 + Q^2/s_0)} \left(1 - \frac{5}{3} \frac{\alpha_s(Q^2)}{\pi} \right), \quad s_0 = 8\pi^2 f_\pi^2 = 0.67 \text{ GeV}^2 \sim m_\rho^2 \quad (31)$$

where the NLO perturbative contribution $\left(-\frac{5}{3} \frac{\alpha_s(Q^2)}{\pi} \right)$ has been added to the original result according to the suggestion of Ref.[9, 18].

The conventional value for the constitute quark mass m is around 0.30 GeV. In the present section, we concentrate our attention on the case of $m = 0.30 \text{ GeV}$ and we will study the uncertainty caused by varying m within a wider region of $[0.20 \text{ GeV}, 0.40 \text{ GeV}]$

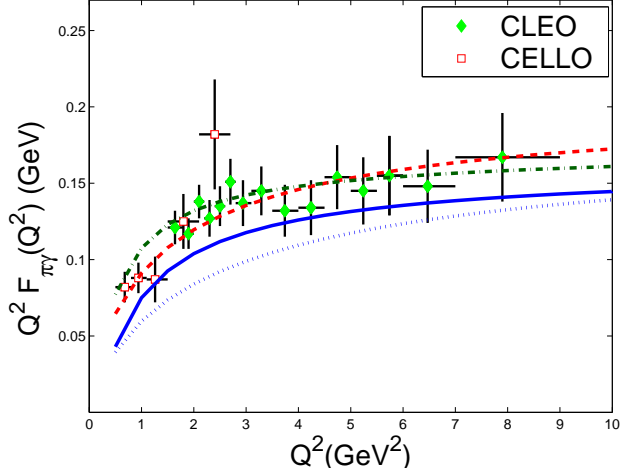


FIG. 4: $Q^2 F_{\pi\gamma}(Q^2)$ that is defined in Eq.(19) and is calculated with the model wavefunction (23) for the case of $m = 0.30$ GeV ($\beta = 0.55$ GeV), which is shown by a dash-dotted line. The dashed line is best fit for the CLEO experimental data [30, 31], the solid line is from the interpolation formula (31) and the dotted line is the results for $Q^2 F_{\pi\gamma}^{(V)}(Q^2)$ only.

in the next section. We show the pion-photon transition form factor $Q^2 F_{\pi\gamma}(Q^2)$ with the model wavefunction (23) for the case of $m = 0.30$ GeV in Fig.(4), where the values for $\beta = 0.55$ GeV and $A = 25.6$ GeV $^{-1}$ can be obtained by using Eqs.(27,30). Fig.(4) shows that by taking the model wavefunction (23) with $m = 0.30$ GeV, the predicted value of $Q^2 F_{\pi\gamma}(Q^2)$ agrees well with the experimental data. We also show the leading Fock-state contribution $Q^2 F_{\pi\gamma}^{(V)}(Q^2)$ in Fig.(4), which is drawn in a dotted line and its value is lower than the experimental data especially in low Q^2 region. As a comparison, we draw the curve for the interpolation formula (31) in Fig.(4), where similar to Ref.[36], we adopt the one loop α_s -running with $\Lambda_{QCD}^{N_f=3} = 312$ MeV to do our calculation. It shows that $Q^2 F_{\pi\gamma}^{BL}(Q^2)$ agrees with the data especially for the low Q^2 region, which is reasonable as the effective value of s_0 in $F_{\pi\gamma}^{BL}(Q^2)$ is determined by the known behavior of $Q^2 \rightarrow 0$.

IV. DISCUSSION AND COMMENT

A. Information of the leading Fock state

As shown in Fig.(4), $F_{\pi\gamma}(Q^2)$ agrees well with the experimental data by taking the leading Fock-state pion wavefunction (23) with $m = 0.30$ GeV. We also show the leading Fock-state

contribution $Q^2 F_{\pi\gamma}^{(V)}(Q^2)$ in Fig.(4), which is lower than the experimental data in low Q^2 region. This shows that one should take into account the higher Fock states in small to intermediate Q^2 region. In fact, it has been found that the leading Fock-state contribution $F_{\pi\gamma}^{(V)}(Q^2)$ fail to reproduce the $Q^2 = 0$ value corresponding to the axial anomaly [5, 7], i.e. it gives only half of what is needed to get the correct $\pi^0 \rightarrow \gamma\gamma$ rate [27]. And to make a compensation, in Refs.[6, 9, 17], the leading Fock-state contribution $F_{\pi\gamma}^{(V)}(Q^2)$ has been enhanced by replacing the leading Fock-state wavefunction to an ‘effective’ valence quark wavefunction that is normalized to one. By taking the ‘effective’ pion wavefunction with the asymptotic-like DAs, the authors found an agreement with the experimental data for $F_{\pi\gamma}(Q^2)$ [6, 9, 17]. However, such an ‘effective’ pion wavefunction is no longer the leading Fock-state wavefunction itself and the probability of finding the leading Fock state in pion should be less than one.

By substituting the pion wavefunction (23) into the pion electro-magnetic form factor, one can obtain some useful information, such as the probability of finding the leading Fock state in pion $P_{q\bar{q}}$, the mean square transverse-momentum of the leading Fock state $\langle \mathbf{k}_\perp^2 \rangle_{q\bar{q}}$ and the charged mean-square-radius $\langle r_{\pi+}^2 \rangle^{q\bar{q}}$. In Refs.[37, 39], the authors have done such a calculation within the LC pQCD approach. By adopting the formulae derived in Ref.[37] (Eqs.(24,25,27) there), one may obtain:

$$P_{q\bar{q}} = 56\%, \quad \langle \mathbf{k}_\perp^2 \rangle_{q\bar{q}} = (0.502 \text{ GeV})^2, \quad \langle r_{\pi+}^2 \rangle^{q\bar{q}} = (0.33 \text{ fm})^2, \quad (32)$$

where we have taken $m = 0.30 \text{ GeV}$. All the values in Eq.(32) are summed results for all the helicity states $\lambda_1 + \lambda_2 = (0, \pm 1)$ of the leading Fock state. Eq.(32) shows that the value of $\langle r_{\pi+}^2 \rangle^{q\bar{q}}$ is smaller than the pion charged radius $\langle r^2 \rangle_{expt}^{\pi^+} = (0.671 \pm 0.008 \text{ fm})^2$ [40], but it is close to the value as suggested in Refs.[37, 41]. Such small $\langle r_{\pi+}^2 \rangle^{q\bar{q}}$ for the leading Fock-state wavefunction is reasonable, since the probability of leading Fock state $P_{q\bar{q}}$ is only 56%, which confirms the necessity of taking the higher Fock-states into consideration to give full estimation of the pion electromagnetic form factor/pion-photon transition form factor, especially for lower Q^2 regions.

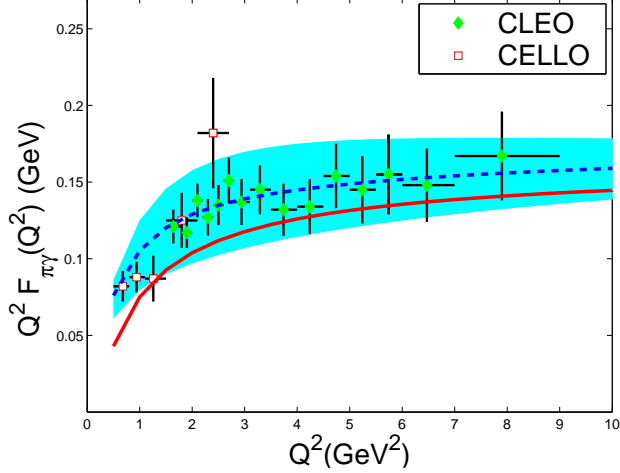


FIG. 5: $Q^2 F_{\pi\gamma}(Q^2)$ with the phenomenological model (20) for $F_{\pi\gamma}^{(NV)}(Q^2)$, with the upper edge of the band for $m = 0.40$ GeV and the lower edge of the band for $m = 0.20$ GeV. The dashed line is the best fit of $Q^2 F_{\pi\gamma}(Q^2)$ for wavefunction (23) with $m = 0.30$ GeV. As a comparison, the interpolation formula (31) is shown by a solid line.

B. Moments of the DA from the CLEO data

In this subsection, we take a wider region for m , i.e. $m = 0.30_{-0.10}^{+0.10}$ GeV, to study the Gegenbauer moments of pion DA. Under such region for m , we show the value of $Q^2 F_{\pi\gamma}(Q^2)$ in Fig.(5). The value of $Q^2 F_{\pi\gamma}(Q^2)$ will increase with the increment of m and the uncertainty caused by varying m within the region of $[0.20 \text{ GeV}, 0.40 \text{ GeV}]$ is about $\pm 20\%$. By comparing Fig.(5) with Fig.(2), it can be found that $m \in (0.20 \text{ GeV}, 0.40 \text{ GeV})$ is a reasonable region for $Q^2 F_{\pi\gamma}(Q^2)$, which is in agreement with the experimental data in the whole Q^2 region.

The pion DA in Eq.(2) can be defined through the matrix elements of local operators between the physical pion and the vacuum state [42, 43]. In the light-cone framework, by choosing the frame in which $P = (1, 0, \mathbf{0}_\perp)$ that has been adopted in Sec.II to calculate the pion-photon transition form factor, its explicit form is given by the following equation [44]:

$$\phi(x_i, Q^2) = \int \frac{dz^-}{2\pi} e^{i(x_1 - x_2)z^-/2} \times \left\langle 0 \left| \bar{u}(-z) \frac{\gamma^+ \gamma_5}{2\sqrt{2}} [-z, z] d(z) \right| \pi(P) \right\rangle_{z^+ = z_\perp = 0}^{(Q^2)}, \quad (33)$$

where the factorization scale is taken to be Q^2 and the path-order factor $[-z, z] = \mathcal{P} \exp \left(ig_s \int_{-1}^1 ds A^+(zs) z^-/2 \right)$ stands for the conventional Wilson line connecting the points $-z$ and z . The line integral vanishes in the light-cone gauge due to $A^+ = 0$. The behavior of $\phi(x_i, Q^2)$ for the large Q^2 is dominated by the behavior of the operator $T(\bar{u}(-z)d(z))$ for

$z^2 = \mathcal{O}(1/Q^2)$. One can apply the usual OPE and only gauge invariant operator that is actually contributes to the matrix element in the light-cone gauge. Therefore only the $q\bar{q}$ component is required in the above definition for the leading power behavior [43]. Also the corresponding higher twist operators of the wave function matrix elements are suppressed at the short distance by power of $1/Q^2$. Thus, the DA $\phi(x_i, Q^2)$ defined in Eq.(33) is the amplitude for finding the $q\bar{q}$ component that is collinear up to the scale Q^2 . On the other hand, the matrix element $\langle 0|\bar{u}\gamma_\mu\gamma_5 d|\pi(P)\rangle$ can be expressed by the following expansion [45]

$$\begin{aligned} \langle 0|\bar{u}(-z)\gamma_\mu\gamma_5[-z, z]d(z)|\pi(P)\rangle^{(Q^2)} = \\ i\sqrt{2}f_\pi P_\mu \int_0^1 du e^{i(2u-1)P\cdot z} \phi_\pi(u, Q^2) + \frac{i}{\sqrt{2}}m_\pi^2 \frac{z_\mu}{P\cdot z} \int_0^1 du e^{i(2u-1)P\cdot z} g_\pi(u, Q^2), \end{aligned} \quad (34)$$

where ϕ_π is the leading twist-2 DA, g_π is the twist-4 DA. Under the light-cone gauge, the DA $\phi(x_i, Q^2)$ defined in Eq.(33) corresponds to the leading twist-2 DA ϕ_π defined in Eq.(34), except for an overall normalization factor. Both definitions are consistent with each other.

We can derive the leading twist-2 pion DA that is in the usual helicity ($\lambda_1 + \lambda_2 = 0$) from Eq.(23), i.e.

$$\phi_\pi(x, \mu_0^2) = \frac{Am\beta\sqrt{3}\sqrt{x(1-x)}}{2\sqrt{2}f_\pi\pi^{3/2}} \left(\text{Erf} \left[\sqrt{\frac{m^2 + \mu_0^2}{8\beta^2 x(1-x)}} \right] - \text{Erf} \left[\sqrt{\frac{m^2}{8\beta^2 x(1-x)}} \right] \right), \quad (35)$$

where the fixed low energy scale μ_0 is taken to be 2 GeV and $\phi_\pi(x, \mu_0^2)$ satisfies the normalization $\int_0^1 \phi_\pi(x, \mu_0^2) dx = 1$. By expanding Eq.(35) into the Gegenbauer polynomials, for $m \in [0.20 \text{ GeV}, 0.40 \text{ GeV}]$, we obtain

$$\begin{aligned} a_2(\mu_0^2) = 0.002_{-0.054}^{+0.063}, \quad a_4(\mu_0^2) = -0.022_{-0.012}^{+0.026}, \\ a_6(\mu_0^2) = -0.014_{+0.000}^{+0.009}, \quad a_8(\mu_0^2) = -0.006_{-0.001}^{+0.003}, \quad \dots, \end{aligned} \quad (36)$$

where the center value is for taking $m \simeq 0.30 \text{ GeV}$ that best fits the CLEO experimental data, i.e. it has the minimum χ^2 -value, and the ellipsis stands for higher Gegenbauer moments. For the values of $a_{2n}(\mu^2)$ in other factorization scales, they can be derived by QCD evolution e.g. Eq.(17). Eq.(36) shows: A) the leading twist-2 pion wavefunction (23) is asymptotic-like, since a_{2n} ($n \geq 1$) are much smaller than $a_0 \equiv 1$. More explicitly, the first inverse moment of the pion DA at energy scale μ_0 , $\int_0^1 dx \phi_\pi(x, \mu_0^2)/x = 3(1 + a_2 + a_4 + a_6 + a_8) \in (2.71, 3.20)$, which is near the same value as for the asymptotic wavefunction with $a_{2n} = 0$ ($n \geq 1$). Such a conclusion for pion wavefunction agrees with that of Ref.[46] and also agrees with a recent

study that is based on the nonlocal chiral-quark model from the instanton vacuum [47]. B) a_2, a_4 will increase with the decrement of m , and $a_2 \geq 0$ if $m \leq 0.30$ GeV. C) the absolute values of a_4, a_6 and a_8 are comparable to a_2 for bigger m (e.g. $m \sim 0.30$ GeV); but they are suppressed to a_2 about one order for smaller m . The value of the Gegenbauer moments have been studied in various processes, cf. Refs.[15, 32, 35, 36, 47, 48, 49, 50, 51, 52, 53]. The lattice result of Ref.[52] prefers a narrower DA with $a_2(1 \text{ GeV}^2) = 0.07(1)$, while the lattice results [50, 51] prefer wider DA, i.e. they obtain $a_2(1 \text{ GeV}^2) = 0.38 \pm 0.23_{-0.06}^{+0.11}$ and $a_2(1 \text{ GeV}^2) = 0.364 \pm 0.126$ respectively. However as argued in Ref.[54], the accuracy of the lattice results needs to be further improved, e.g. the results in Ref.[51] for the second moment $\langle \xi^2 \rangle$ are obtained for the “pion” with the masses $\mu_\pi > 550$ MeV and then extrapolated to the chiral limit $\mu_\pi \rightarrow 0$. These references favor a positive value for $a_2(1 \text{ GeV}^2)$ and the most recent one is done by Ref.[49], which shows that $a_2(1 \text{ GeV}^2) = 0.19 \pm 0.19$ and $a_4(1 \text{ GeV}^2) \geq -0.07$ by analyzing the leptonic mass spectrum of $B \rightarrow \pi l \nu$. Here, the range of m should be reduced to $m \in [0.20 \text{ GeV}, 0.30 \text{ GeV}]$ if we require $a_2(1 \text{ GeV}^2) \geq 0$ for the pion DA. Or inversely, we have $a_2(1 \text{ GeV}^2) \in [0, 0.08]$ with the help of the QCD evolution equation (17) for $m \in [0.20 \text{ GeV}, 0.30 \text{ GeV}]$.

C. Comparison with the broad wavefunction

One typical broad wavefunction is described by the CZ-like wavefunction, which can not be excluded by the pion-photon transition form factor [5] although it is disfavored by the pion structure function at $x \rightarrow 1$ [28].

We take the CZ-like wavefunction as

$$\Psi_{q\bar{q}}^{CZ}(x, \mathbf{k}_\perp) = A(1 - 2x)^2 \exp \left[-\frac{\mathbf{k}_\perp^2 + m^2}{8\beta^2 x(1 - x)} \right] \chi^K(x, \mathbf{k}_\perp), \quad (37)$$

where an extra factor $(1 - 2x)^2$ is introduced into the pion wavefunction (23) [3]. Following a similar procedure, we find that the relation between m and β changes to

$$6.00 \frac{m\beta}{f_\pi^2} \cong 1.24 \left(\frac{m}{\beta} + 2.12 \right) \left(\frac{m}{\beta} + 4.58 \times 10^1 \right). \quad (38)$$

Similarly, for $m = 0.30$ GeV, we have

$$P_{q\bar{q}} = 73\%, \quad \langle \mathbf{k}_\perp^2 \rangle_{q\bar{q}} = (0.496 \text{ GeV})^2, \quad \langle r_{\pi^+}^2 \rangle^{q\bar{q}} = (0.45 \text{ fm})^2, \quad (39)$$

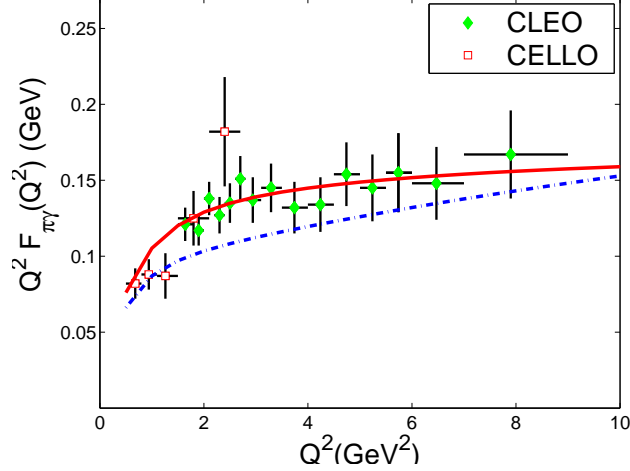


FIG. 6: Comparison of $Q^2 F_{\pi\gamma}(Q^2)$ that is derived from two different types of wavefunctions, i.e. the BHL-like wavefunction (the solid line) and the CZ-like wavefunction (the dash-dotted line), under the condition of $m = 0.30$ GeV.

where all the values are summed results for all the helicity states $\lambda_1 + \lambda_2 = (0, \pm 1)$ of the leading Fock state. One may observe that the second Gegenbauer moment a_2 is always dominant over other higher Gegenbauer moments for the CZ-like DA. And for the first inverse moment of the CZ-like pion DA at energy scale μ_0 , we obtain $\int_0^1 dx \phi_\pi^{CZ}(x, \mu_0^2)/x = 4.69$.

In Fig.(6), we make a comparison of $Q^2 F_{\pi\gamma}(Q^2)$ that is derived from two different types of wavefunctions, i.e. the BHL-like wavefunction and the CZ-like wavefunction, under the same value of $m = 0.30$ GeV. Both the BHL-like wavefunction and the CZ-like wavefunction lead to $Q^2 F_{\pi\gamma}(Q^2)$ within the possible region of the experimental data as shown in Fig.(2). However, the value of $Q^2 F_{\pi\gamma}(Q^2)$ derived from the BHL-like wavefunction is better than that of the CZ-like wavefunction. One may observe that the value of $Q^2 F_{\pi\gamma}(Q^2)$ caused by the CZ-like wavefunction shall increase with the increment of m , so the CZ-like model can give a better result for $Q^2 F_{\pi\gamma}(Q^2)$ in comparison to the experimental data only by taking a bigger value for m , e.g. at least, $m = 0.40$ GeV.

As a summary, the main differences for the BHL-like wavefunction and the CZ-like wavefunction are listed in the following:

- By comparing with the experimental data for $Q^2 F_{\pi\gamma}(Q^2)$, one may observe that $m = 0.30^{+0.10}_{-0.10}$ GeV is a reasonable region for the BHL-like wavefunction, where the best fit to the experimental data is achieved when $m \approx 0.30$ GeV; while for the case of the

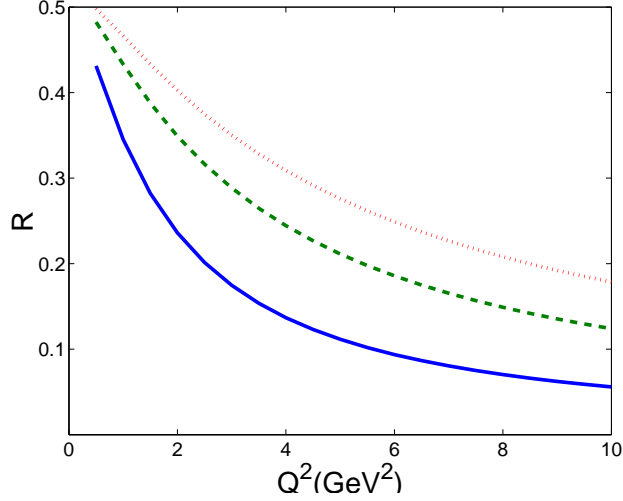


FIG. 7: The value of $R = \frac{F_{\pi\gamma}^{(NV)}(Q^2)}{F_{\pi\gamma}^{(V)}(Q^2) + F_{\pi\gamma}^{(NV)}(Q^2)}$ versus Q^2 for the BHL-like wavefunction, whose value increases with the increment of m . The solid, dashed and dotted lines are for $m = 0.20\text{GeV}$, $m = 0.30\text{GeV}$ and $m = 0.40\text{GeV}$, respectively.

CZ-like wavefunction, such region is shifted to a higher one, i.e. $m = 0.40^{+0.10}_{-0.10}$ GeV, and the best fit to the experimental data is achieved as $m \approx 0.40$ GeV, which is somewhat bigger than the conventional value for the constituent quark mass of pion.

- The difference among the Gegenbauer moments e.g. $a_2(\mu_0^2)$ are big due to the different behavior of the two models. Under the condition of $m = 0.30$ GeV, the two Gegenbauer moments $a_2(\mu_0^2) = 0.002$ and $a_4(\mu_0^2) = -0.022$ for the BHL-like model (20); while for the CZ-like model (37), $a_2(\mu_0^2) = 0.678$ and $a_4(\mu_0^2) = -0.024$.
- The first inverse moments are different. Under the condition of $m = 0.30$ GeV, for the case of the BHL-like model (20), $\int_0^1 dx \phi_{\pi}^{BHL}(x, \mu_0^2)/x = 2.88$, which is close to that of the asymptotic DA; while for the case of the CZ-like model (37), $\int_0^1 dx \phi_{\pi}^{CZ}(x, \mu_0^2)/x = 4.69$, which is close to that of the original CZ-model [3].

In Ref.[54], it was shown that by taking the asymptotic DA and considering the suppression from the NLO contribution, the value of $Q^2 F_{\pi\gamma}(Q^2)$ at $Q^2 = 8.0$ GeV² is somewhat smaller than the experimental value $(16.7 \pm 2.5 \pm 0.4) \cdot 10^{-2}$ GeV, i.e. $Q^2 F_{\pi\gamma}(Q^2)|_{Q^2=8.0 \text{ GeV}^2} \simeq 0.115$ GeV. However it should be pointed out that Ref.[54] is only a simplified analysis, since the effects caused by the k_T -dependence in both the pion wavefunction and the hard scattering amplitude, and the contribution from $F_{\pi\gamma}^{(NV)}(Q^2)$ have not been taken into consideration.

As shown in Fig.(7), even though $F_{\pi\gamma}^{(NV)}(Q^2)$ is suppressed to $F_{\pi\gamma}^{(V)}(Q^2)$ in high Q^2 region, it has sizable contribution in the intermediate Q^2 region, e.g. it is about 12% at $Q^2 = 8.0 \text{ GeV}^2$ for the case of $m = 0.30 \text{ GeV}$.

D. A simple discussion of the NLO correction

Up to NLO, by taking the square of the factorization scale μ_F^2 to be Q^2 , the pion-photon transition form factor $F_{\pi\gamma}(Q^2)$ can be schematically written as

$$F_{\pi\gamma}(Q^2) = F_{\pi\gamma}^{(V)}(Q^2) \left(1 - \delta \cdot \frac{\alpha_s(Q^2)}{\pi} \right) + F_{\pi\gamma}^{(NV)}(Q^2), \quad (40)$$

where δ is a parameter that is to be determined by the behavior of the pion wavefunction/DA and the detail form of the hard scattering amplitude. It is a natural choice to take $\mu_F^2 = Q^2$, which directly eliminates the μ_F -dependence in the terms that determine how much of the collinear term is absorbed into the distribution amplitude [10, 15]. In the literature, the value of δ has been estimated to be: $\delta = \frac{5}{3}$ for asymptotic DA [9, 10, 18] and $\delta = \frac{49}{108}$ for DA in CZ form [9]. It should be noted that to be consistent with our present calculation technology, we need a full NLO result, in which all the effects caused by the transverse-momentum dependence in the hard-scattering amplitude and the wavefunction and by the Sudakov factor should be fully taken into consideration. However such a full NLO calculation is not available at the present. The value of δ will be decreased by considering the transverse-momentum dependence in the hard-scattering amplitude and the wavefunction (a naive discussion for this point can be found in Refs.[9, 11]). Since our model wavefunction is close to asymptotic-like one, we simply take $\delta = \frac{5}{3}$ to do our discussion.

Under the condition of $\delta = \frac{5}{3}$, it can be found that the best fit of $Q^2 F_{\pi\gamma}(Q^2)$ for the case of the BHL-like wavefunction (23) is at $m \simeq 0.32 \text{ GeV}$. If taking $m = 0.32 \pm 0.10 \text{ GeV}$, we obtain $a_2(\mu_0^2) = -0.02_{-0.08}^{+0.07}$, where $\mu_0 \simeq 2 \text{ GeV}$. Furthermore, if taking $a_2(1 \text{ GeV}^2) > 0$ as an extra constraint, we find that m must be in the region of $[0.23, 0.30] \text{ GeV}$. Or inversely, we have $a_2(1 \text{ GeV}^2) \in [0, 0.06]$ for $m \in [0.23 \text{ GeV}, 0.30 \text{ GeV}]$.

V. SUMMARY

In this paper, we have given a careful analysis of the pion-photon transition form factor $F_{\pi\gamma}(Q^2)$ involving the transverse momentum corrections with the present CLEO experimen-

tal data, in which the contributions beyond the leading Fock state have been taken into consideration. As is well-known, the leading Fock-state contribution dominates the pion-photon transition from factor $F_{\pi\gamma}(Q^2)$ for large Q^2 region and it gives only half contribution to $F_{\pi\gamma}(0)$ as one extends it to $Q^2 = 0$. One should consider the higher Fock states' contribution to $F_{\pi\gamma}(0)$ at the present experimental Q^2 region. We have constructed a phenomenological expression to estimate the contributions beyond the leading Fock state based on the limiting behavior of $F_{\pi\gamma}^{(NV)}(Q^2)$ at $Q^2 \rightarrow 0$. The calculated results favor the asymptotic-like behavior by comparing the predictions from different type of the model wavefunctions with the experimental data.

On the other hand, the present CLEO data provides the important information of the pion DA as one has a complete expression for the pion-photon transition form factor relates two photons with one pion. Our expression for $F_{\pi\gamma}(Q^2)$ only involves a single pion DA. Thus, comparing the calculated results of $F_{\pi\gamma}(Q^2)$ by taking the BHL-like pion wavefunction with the CLEO data one can extract some useful information of the pionic leading twist-2 DA. Our analysis shows that (1) the probability of finding the leading Fock state in the pion is less than one, i.e. $P_{q\bar{q}} = 56\%$ and $\langle r_{\pi^+}^2 \rangle^{q\bar{q}} = (0.33 \text{ fm})^2$ with $m = 0.30 \text{ GeV}$. This means that the leading Fock state is more compact in the pion and it is necessary to take the higher Fock states into account to give full estimation of the pion-photon transition form factor and other exclusive processes. (2) under the region of $m \in [0.20 \text{ GeV}, 0.40 \text{ GeV}]$, we have the DA moments: $a_2(\mu_0^2) = 0.002_{-0.054}^{+0.063}$, $a_4(\mu_0^2) = -0.022_{-0.012}^{+0.026}$ and all of higher moments. Such result is helpful to understand other exclusive processes involving the pion.

ACKNOWLEDGEMENTS

This work was supported in part by the Natural Science Foundation of China (NSFC). X.-G. Wu thanks the support from the China Postdoctoral Science Foundation.

-
- [1] G.P. Lepage and S.J. Brodsky, Phys.Rev.**D22**, 2157(1980); S.J. Brodsky and G.P. Lepage, Phys.Rev.**D24**, 1808(1981).
 - [2] Particle Data Group, E.J. Weinberg, *et al.*, Phys.Rev. **D66**, 010001(2002).
 - [3] V.L. Chernyak and A.R. Zhitnitsky, Nucl.Phys. **B201**, 492(1982).

- [4] S.J. Brodsky, T. Huang and G.P. Lepage, in *Particles and Fields-2*, Proceedings of the Banff Summer Institute, Banff, Alberta, 1981, edited by A.Z. Capri and A.N. Kamal (Plenum, New York, 1983), P143; T. Huang, in *Proceedings of XXth International Conference on High Energy Physics*, Madison, Wisconsin, 1980, edited by L.Durand and L.G. Pondrom, AIP Conf.Proc.No. 69(AIP, New York, 1981), p1000.
- [5] Fu-Guang Cao, Tao Huang and Bo-Qiang Ma, Phys.Rev. **D53**, 6582(1996).
- [6] Bo-Wen Xiao and Bo-Qiang Ma, Phys.Rev. **D68**, 034020(2003).
- [7] R. Jakob *etal.*, J.Phys. **G22**, 45(1996); P. Kroll and M. Raulfs, Phys.Lett. **B387**, 848(1996).
- [8] A.V. Radyushkin and R. Ruskov, Nucl.Phys. **B481**, 625(1996).
- [9] I.V. Musatov and A.V. Radyushkin, Phys.Rev. **D56**, 2713(1997).
- [10] B. Melic, B. Nizic and K. Passek, Phys.Rev. **D65**, 053020(2002); F. Del Aguila and M.K. Chase, Nucl.Phys. **B193**, 517(1981); E. Braaten, Phys.Rev. **D28**, 524(1983).
- [11] N.G. Stefanis, W. Schroers and H.-Ch. Kim, Eur.Phys.J. **C18**, 137(2000).
- [12] S. Ong, Phys.Rev. **D52**, 3111(1995).
- [13] Tao Huang and Qi-Xing Shen, *Proceedings of the international seminar of Quark'90*, Telavi, USSR, (1990), Ed. by Matveev *etal.*, page 340; Z.Phys. **C50**, 139(1991).
- [14] J. Boots and G. Sterman, Nucl.Phys. **B325**, 62(1989); H.N. Li and G. Sterman, Nucl.Phys. **B381**, 129(1992).
- [15] A.P. Bakulev, K. Passek-Kumericki, W. Schroers and N.G. Stefanis Phys.Rev. **D70**, 033014(2004); Erratum-ibid.**D70**, 079906(2004).
- [16] T.W. Yeh, Phys.Rev. **D65**, 074016(2002).
- [17] A.V. Radyushkin, Acta Phys.Polon. **B26**, 2067(1995); hep-ph/9511272.
- [18] S.J. Brodsky, C.R. Ji, A. Pang and D.G. Robertson, Phys.Rev. **D57**, 245(1998).
- [19] G.P. Lepage, S.J. Brodsky, T. Huang and P.B. Mackenzie, in *Particles and Fields-2*, page 83, Invited talk presented at the Banff summer Institute on Particle Physics, Banff, Alberta, Canada, 1981.
- [20] S.J. Brodsky, H.C. Pauli and S.S. Pinsky, Phys.Rept. **301**, 299(1998); and references therein.
- [21] S.D. Drell and T.M. Yan, Phys.Rev. Lett.**24**, 181(1970); G.B. West, Phys.Rev. Lett.**24**, 1206(1970).
- [22] K. Wilson, Phys.Rev. **179**, 1499(1969); R. Brandt and G. Preparata, Nucl.Phys. **B27**, 541(1971); N. Christ, B. Hasslacher and A.H. Mueller, Phys.Rev. **D6**, 3543(1972).

- [23] H.B. O'Connell, B.C. Pearce, A.W. Thomas and A.G. Williams, *Prog.Part.Nucl.Phys.* **39**, 201(1997).
- [24] J.P.B.C. de Melo, T. Frederico, E. Pace and G. Salme, *Phys.Lett.* **B581**, 75(2004);
- [25] J.P.B.C. de Melo, T. Frederico, E. Pace and G. Salme, *Phys.Rev.* **D73**, 074013(2006).
- [26] T. Draper, R.M. Woloshyn, W. Wilcox and K. Liu, *Nucl.Phys.* **B318**, 319(1989).
- [27] S. Treiman, R. Jackiw and D. Gross, *Lectures on the Current Algebra and its Applications*, Princeton University Press (Princeton, 1972).
- [28] T. Huang, B.Q. Ma and Q.X. Shen, *Phys.Rev.* **D49**, 1490(1994).
- [29] Dieter Muller, *Phys.Rev.* **D51**, 3855(1995).
- [30] CLEO collaboration, V. Savinov *et al.*, hep-ex/9707028; CLEO Collaboration, J. Gronberg *et al.*, *Phys.Rev.* **D57**, 33(1998).
- [31] CELLO collaboration, H.-J. Behrend *et al*, *Z.Phys.* **C49**, 401(1991).
- [32] A. Schmedding and O. Yakovlev, *Phys.Rev.* **D62**, 116002(2000).
- [33] A.E. Dorokhov, *JETP Lett.* **77**, 63(2003); hep-ph/0212156.
- [34] W.H. Press, S.A. Teukolsky, W.T. Vetterling and B.P. Flannery, *Numerical Recipes in Fortran 77: The Art of Scientific Computing, Second Editon*, Published by the Press Syndicate of the University of Cambridge (1992), p650.
- [35] A.P. Bakulev, S.V. Mikhailov and N.G. Stefanis, *Phys.Lett.* **B578**, 91(2004).
- [36] A.P. Bakulev, S.V. Mikhailov and N.G. Stefanis, *Phys.Rev.* **D67**, 074012(2003); *Phys.Rev.* **D73**, 056002(2006).
- [37] Tao Huang, Xing-Gang Wu and Xing-Hua Wu, *Phys.Rev.* **D70**, 053007(2004); Xing-Gang Wu and Tao Huang, *Int.J.Mod.Phys.* **A21**, 901(2006).
- [38] Tao Huang and Xing-Gang Wu, *Phys.Rev.* **D70**, 093013(2004).
- [39] F. Cardarelli, *etal.*, *Phys.Rev.* **D53**, 6682(1996).
- [40] S.R. Amendolia, *etal.*, *Phys.Lett.* **B146**, 116(1985).
- [41] B. Povh and J. Hufner, *Phys.Lett.* **B245**, 653(1990); T. Huang, *Nucl.Phys. (Proc. Suppl.)* **7**, 320(1989).
- [42] A.V. Radyushkin, hep-ph/0410276.
- [43] S.J. Brodsky, Y. Frishman and G.P. Lepage, *Phys.Lett.* **B91**, 239(1980).
- [44] S.J. Brodsky, P. Damgaard, Y. Frishman and G.P. Lepage, *Phys.Rev.* **D33**, 1881(1986).
- [45] P. Ball, *J. High Energy Phys.* **9901**, 010(1999).

- [46] P. Kroll and M. Raulfs, Phys.Lett. **B387**, 848(1996); A.P. Bakulev, S.V. Mikhailov, N.G. Stefanis, Phys.Lett. **B508**, 279(2001), Erratum: *ibid* **B590**, 309(2004).
- [47] Seung-il Nam, Hyun-Chul Kim, Atsushi Hosaka and M. M. Musakhanov, hep-ph/0605259.
- [48] V.M. Braun, A. Khodjamirian and M. Maul, Phys.Rev. **D61**, 073004(2000).
- [49] P. Ball and R. Zwicky, Phys.Lett. **B625**, 225(2005).
- [50] L. Del Debbio, M. Di Perro and A. Dougall, Nucl.Phys.Proc.Suppl. **119**, 416(2003).
- [51] M. Gockeler, *et al* hep-lat/0510089.
- [52] S. Dalley and Brett van de Sande, Phys.Rev. **D67**, 114507(2003).
- [53] S.S. Agaev, Phys.Rev. **D72**, 114010(2005); Erratum-ibid. **D73**, 059902(2006).
- [54] V.L. Chernyak, hep-ph/0605327.